Physics – Uspekhi **63** (5) 487 – 499 (2020)

INSTRUMENTS AND METHODS OF INVESTIGATION PACS numbers: **34.35.+a, 37.20.+j**

Desorption processes in the measurement of weak currents

V G Lukin, O G Khvostenko

DOI: https://doi.org/10.3367/UFNe.2019.07.038615

Contents

Abstract. It was previously shown that the experimental measurement of the lifetime of gas-phase negative ions formed in autoionization states during resonant electron capture by molecules is inherently fraught with inaccuracy due to adsorption of ions on the walls of the ionization chamber, with some of them surviving there and staying stabilized as 'eternal' till they eventually desorb back into the vacuum and merge with the total ion flow; this leads to an upward distortion of lifetime measurements. This paper describes a technique for removing desorbed ions from the total flow using an ion filter that lets only gas-phase ions pass into the detection system but detains the desorbed ions due to the differences among their kinetic energies.

Keywords: resonant electron capture, lifetime of negative ions, temperature dependence, ion adsorption, mass spectrometry

1. Introduction

Autodetachment states of negative ions (NIs) formed in a high vacuum as a result of resonant electron capture (REC) by molecules have for many decades been a focus of extensive research carried out with the use of various experimental and theoretical methods [1–15] the results of which are important for understanding physical processes underlying the electron-matter interaction, of which REC is an elementary act free from the influence of circumstantial factors. REC studies are of equal value for a variety of applications due to the involvement of NIs in many natural and artificial physicochemical processes [16, 17]. For example, it is well known that, the formation of oxygen negative ions affects the ionosphere determining the free electron concentration, aurora spectrum, and night airglow. In Earth's atmosphere, these ions contribute to the formation of conductive plasma, which can trigger a lightning in the case of electrical breakdown in the air. The absorption of hydrogen NIs in the Sun's atmosphere determines the solar spectral irradiance distribution. The formation, destruction, and recombination of negative ions promote radiochemical reactions and affect the operation of Geiger–Müller counters and electron-beam tubes. Moreover, NIs take part in electron transfer in photosystems and charge separation in photoelectric cells [18–20] and reduce medium conductivity in gases and plasma due to an additional channel of electron loss as a result of joining to electronegative molecules present there. A fall of conductivity is due to a lower thermal velocity of ions than that of electrons as exemplified by sulfur hexafluorde (SF_6), a compound best explored by REC methods.

Due to high electronegativity manifesting itself in a large cross section for the capture of free electrons and high ionization energy, SF_6 is widely used in high-voltage power engineering and gas-discharge devices. In basic research, it is used as a benchmark to calibrate electron energy scales and control electron energy (E_{el}) distribution in REC experiments, bearing in mind that an SF_6 molecule produces NIs as it traps electrons with a strictly zero energy [9].

Another equally well-known compound thoroughly investigated by the REC technique is nitrobenzene ($C_6H_5NO_2$), widely used in chemical technologies to manufacture aniline, other aromatic nitrogen-containing compounds, paint-and-lacquer materials, explosives, and rocket-engine propellant, as well as in such 'peaceful' industries as perfumery and medicine (by virtue of the same electron-accepting properties as in SF_6). The high demand for $C_6H_5NO_2$ and SF_6 for a variety of purposes accounts for the choice of these compounds in numerous studies designed to address the problem of measuring the lifetime of negative ions, as described below in this article.

V G Lukin (*), **O G Khvostenko**
Institute of Molecular and Crystal Physics — Subdivision of the Ufa Federal Research Center, Russian Academy of Sciences, prosp. Oktyabrya 151, 450075 Ufa, Russian Federation
E-mail: (*) Lukin@anrb.ru

Received 11 April 2019, revised 19 June 2019
Uspekhi Fizicheskikh Nauk **190** (5) 525 – 538 (2020)
Translated by Yu V Morozov; edited by V L Derbov

The lifetime τ_a of a negative molecular ion $^aM^-$ formed during REC, with respect to autodetachment of an extra electron, is one of its most important characteristics. Values of τ_a fall into an extremely broad range (11 orders of magnitude or greater) that extends from picoseconds to microseconds due to a diversity of mechanisms underlying the formation and decay of $^aM^-$ ions. Of primary importance in this context is the relative position of the parent molecule and negative ion potential surfaces, their electronic terms [11, 12]. The mechanism of extra electron capture by a molecule, its residence time in the trap, and the autodetachment mechanism are closely related to whether the ion energy term is above or below the molecule term and to intersection of terms in the molecule equilibrium geometry region. If the ion term is above the molecule term, the ion is likely to form by uptake of an electron with a higher than zero kinetic energy ($E_{el} > 0$), equaling the energy distance between molecule and ion terms in the vertical transition region. Under these conditions, any of the three possible REC mechanisms can be realized, viz. shape resonance (SR) [8, 14], electron-excited Feshbach resonance (EER) [1, 10], and inter-shell resonance (ISR) [21, 22]. In all these cases, ions have doublet multiplicity ($^2M^-$) and short lifetimes of $10^{-15}-10^{-10}$ s. Such lifetimes can not be measured and are estimated theoretically.

Nevertheless, in certain rare cases when the ion term is above the molecule one, ions can form at $E_{el} > 0$ but with longer lifetimes (a few microseconds), the cause being $^2M^- \to {}^4M^-$ doublet-quartet intersystem crossing, responsible for the generation of ions with quartet multiplicity ($^4M^-$) having three unpaired electrons with identically directed spins. One of them is additional, while the other two are electrons of the parent molecule in a triplet configuration. The autodetachment of the extra electron from such an ion is delayed by the spin ban, consisting of the fact that the molecule must remain in the ground electronic state, as opposed to the triplet one, after the extra electron is expelled from the 'quartet' ion, because the triplet energy is higher than the ion energy. This condition implies that at the instant of ejection of the extra electron, the excited (triplet) electron must fill the vacancy at a lower molecular level ('fall down'), i.e., move to the level containing the third unpaired electron with the same spin. Naturally, this must be accompanied by spin inversion of the 'falling' electron. The necessity of such inversion delays the entire process, including emission of the extra electron from the ion and prolonging its lifetime up to a few microseconds [23–25]. The microsecond range of τ_a available for measurements allows instrumental determination of the lifetime of $^4M^-$-like and other long-lived negative ions for which $\tau_a \geqslant 10^{-6}$ s (see below).

When the ion term is below the molecule term (positive electron affinity of the molecule) and intersects it in the molecule equilibrium geometry region, one more (much broader) class of long-lived NI is likely to form. The mechanism of their formation is known as vibrationally excited Feshbach resonance (VEFR). Ions generated by the VEFR mechanism are 'ordinary' $^2M^-$ doublets with the extra electron autodetachment delay attributable to causes other than those behind the delay of $^4M^-$-like ions. In this case, the long lifetime of an ion is a result of transition of the electron affinity energy and the kinetic energy of an incoming electron into kinetic energy of nuclei as a consequence of violation of the Born–Oppenheimer principle. The nuclear subsystem undergoes strong vibrational excitation, its configuration changes, and to expel the extra electron from the ion the nuclei must return to the initial state in which electron capture occurred [1, 10, 12]. However, the return takes time: the more vibrational degrees of freedom the molecule has, the longer it takes. This means that τ_a in VEFR is critically dependent on the number of vibrational degrees of freedom in the system, as shown in [12] based on the statistical Rice–Ramsperger–Kassel–Marcus theory. The same dependence ensues from experimental data for molecular ions of various substances, summarized in Table 3 of Ref. [12]. It demonstrates that the value of τ_a of a negative ion increases as the molecule becomes increasingly complicated. For example, $\tau_a = 7$ μs for SF_4 and $\tau_a = 790$ μs for C_7F_{14}.

It should be noted that the list of substances producing long-lived negative molecular ions included in Table 3 [12] is rather short in comparison with the total number of compounds investigated by REC methods, because not all, but just a few, molecules can give rise to long-lived ions, meaning that the substances included in Table 3 [12] are in a sense exotic, with SF_6 and $C_6H_5NO_2$ among them representing the study subjects in the present paper. They hold a special place, even in the above short list, being of great interest for researchers, as is confirmed by the large number of published REC studies.

Measurements of the lifetime of $^aM^-$ negative ions regarded as long-lived in the context of REC processes, i.e., ions for which $\tau_a \geqslant 10^{-6}$ s, were made throughout the entire period of REC studies by many research groups using various compounds. However, experimenters interested in determining τ_a encountered difficulties related to the interpretation of the wide scatter of τ_a values; they were reported by both different authors and the same authors using the same equipment at different times. Sometimes, the scatter in the measured values of τ_a was so prominent that it generated the order-of-magnitude difference between them (e.g., for SF_6). Such great scatter was reported by Odom and co-workers, who used an ion cyclotron resonance mass spectrometer and obtained $\tau_a(SF_6^-)$ values spanning the range from 50 to 10^4 μs, depending on the experimental conditions [26]. Similar results were reported for SF_6^- and $C_6F_6^-$ ions in a Rydberg electron transfer study using a Penning trap [27] and for $\tau_a(SF_6^-)$ in experiments with the use of the ELectrostatic Ion-Storage ring, Aarhus (ELISA) [28]. The measured $\tau_a(SF_6^-)$ values in experiments with a cryogenic ion beam trap were found to lie in the millisecond range [29]. Analogous observations were made in experiments with other compounds.

Various hypotheses were forwarded to explain the differences among experimental τ_a values, a subject of wide speculation in the literature. It was argued that the scatter may be due to irregular focusing of charged and neutral particles [30], different conditions in ion sources, and their characteristics, including electron energy [31], pressure [32], temperature [33], and luminosity [34]. However, further studies failed to confirm the relevance of the proposed explanations. In the end, the scatter of τ_a values was addressed in the light of the so-called multiexponentiality hypothesis [35]. The validity of this approach was later confirmed in Refs [36, 37]. Today, it is the most widely accepted.

The concept of multiexponentiality postulates that molecules present in an ionization chamber (IC) have a temperature T_{IC} and are distributed over vibrational levels. The higher the vibrational excitation of the initial molecule, the shorter the lifetime of the ions originating from it. Therefore, the total flux of the beam ions that reach the detection system contains ions

with various lifetimes. This phenomenon gave rise to the term multiexponentiality, meaning that ions with different values of τ_a decay (expel an electron) in accordance with different exponential laws. Ions travel different paths from the IC to the detection system in different scientific instruments. Therefore, it takes them different amounts of time to cover the distance. In other words, the instruments have different time windows Δt. As a result, detection systems in different instruments are reached by ions with different lifetimes, which accounts for the scatter of measured τ_a values.

Thus, the multiexponentiality concept implies that the measured ions' lifetime is a function of two parameters, one being the time window of the instrument Δt, the other IC temperature T_{IC}. The latter parameter is of special importance, since it is well known from practical experience that τ_a values of a given compound measured by the same instrument tend to be different, even if the time window Δt remains unaltered. In such a case, the scatter can be theoretically related to the poor control of T_{IC} during the experiment. Moreover, the relevance of the multiexponentiality concept is directly confirmed by the fairly well proven temperature dependence of τ_a: the higher T_{IC}, the shorter τ_a.

However, the latest studies [38–41] have provided data challenging the validity of interpretation of the temperature dependence of τ_a in terms of the multiexponentiality concept. Specifically, τ_a was found to equally decrease at constant T_{IC} if helium was puffed into the ionization chamber. This and some other observations give evidence that the scatter of measured τ_a values may be due to partial adsorption of gas-phase $^aM^-$ ions on the IC surface. It was shown that part of the $^aM^-$ ions formed during REC in the gaseous phase are adsorbed on the IC walls, with some of them undergoing neutralization as expected. However, those ions that avoid neutralization survive and become stabilized on the IC walls up to an 'ever-living' state. After a certain lapse of time, these ions desorb back into the vacuum, till they eventually merge with the total ion flow directed toward the detection system. However, they are unable to detach the extra electron, because their lifetime is 'infinitely long' compared with the electron detachment time ($\tau_a = \infty$). As a result, their arrival at the detection system together with autodetachment gas-phase $^aM^-$ ions that come directly from the IC bypassing its surface causes an upward distortion of lifetime measurements of the $^aM^-$ autodetachment ions. In the case of helium inflow into the IC, the gas cleans its surface and thus promotes ion neutralization, reducing the fraction of desorbed 'eternal' ions joining the total flow and thereby decreasing the measured τ_a value.

It follows from the above that ions absorbed on the surface and desorbed thereafter into the vacuum should be prevented, if possible, from entering the total ion flow to enable correct experimental measurements of τ_a. To address this issue, we introduced a special filter into the ion source of our mass-spectrometer that separated two types of ions ('purely' gas-phase and 'eternal' ones desorbed from the surface), taking advantage of the difference between their kinetic energies. A method developed for this purpose is briefly described in Ref. [42] and presented in more detail in Section 4.

One of the objectives of the present work was also to verify the validity of the multiexponentiality concept with special reference to its main argument, i.e., the form of temperature dependence of τ_a. Clearly, for the concept to be true, this dependence must hold after the removal of ions desorbed from the surface. However, the dependence must disappear after the removal of desorbed ions if ion adsorption-desorption is the key factor responsible for the scatter of measured τ_a values. Therefore, we measured τ_a values at different temperatures using an ion filter (see above) for both SF_6 and $C_6H_5NO_2$.

Studies of surface adsorption and desorption and NIs of complex molecules in this work may be of interest in a broader perspective for the understanding of substance-surface interactions, including charge transfer via the surface, energy exchange between an incident particle and the surface, and ion exchange [43–45], bearing in mind a wide range of practical applications from gas storage and separation, manufacturing chemical detectors, catalysis, drug delivery, and chemical protection to space exploration [46–49]. Adsorption and desorption of neutral atoms, molecules, and radicals are among the most important aspects of matter-surface interaction. Results of this work can be used to analyze such neutral desorbing particles, because ionization makes them easier to detect, as was shown in laboratory experiments designed to simulate gas desorption processes in interstellar dust clouds [50].

2. Mass-spectrometer of negative ions operating in the mode of resonance capture of electrons by molecules

This work was carried out with the use of an MI-1201B static sector mass-spectrometer modified to record NIs in the REC mode. Its functional block diagram is presented in Fig. 1a. It incorporates a Nira-type ion source (IS) characterized by enhanced transmission efficiency and the possibility of changing its technical characteristics [34] (Fig. 1b). The REC spectrum in this and analogous instruments is formed by an electromagnetically collimated electron beam with energy E_{el} varied in a range from 1–15 eV that enters the ionization chamber (IC in Fig. 1a) containing vapors of the study substance whose molecules capture electrons at certain E_{el} values. Negative ions formed in an IC leave it under the action of the repelling electrode electric field (RE in Fig. 1a and *7* in Fig. 1b) to find themselves in the field of the extracting electrode (EE) placed above the exit slit in the IC cap. The ions pulled out from the source are accelerated and enter the first field-free region (FF_1), after which they pass through the mass-analyzer (EM in Fig. 1a). Then, they are separated according to their mass numbers m/z and pass through the second field-free region (FF_2) to be recorded by the secondary electron multiplier (SEM). FF_1 and FF_2 are regions free from electric and magnetic fields (Fig. 1a).

The REC spectrum is recorded in two steps. First, the mass-spectrum is recorded as a set of m/z values; then, the effective yield curve (EYC) is recorded for ions of each m/z as a function of intensity from E_{el}. In the present paper, the width of the electron energy distribution at the half-height of EYC for SF_6 ions was $E_{el} \approx (0.3-0.4)$ eV, electron current ~ 1 μA, accelerating voltage 4 kV. E_{el} scale linearity was calibrated based on EYC maxima ($E_{el} = 0$ eV) for SF_6^- from SF_6 and $C_6H_5^-$ ($E_{el} = 0.8$ eV) from C_6H_6. Constant pressure during puffing was maintained by continuous evacuation. The pressure inside the main vacuum chamber was measured by an ionization manometer; it did not exceed 10^{-6} Pa as was necessary to meet the condition of single collisions in the IC. To exclude undesirable events associated with dielectric film formation [51] and secondary emission electrons reflected

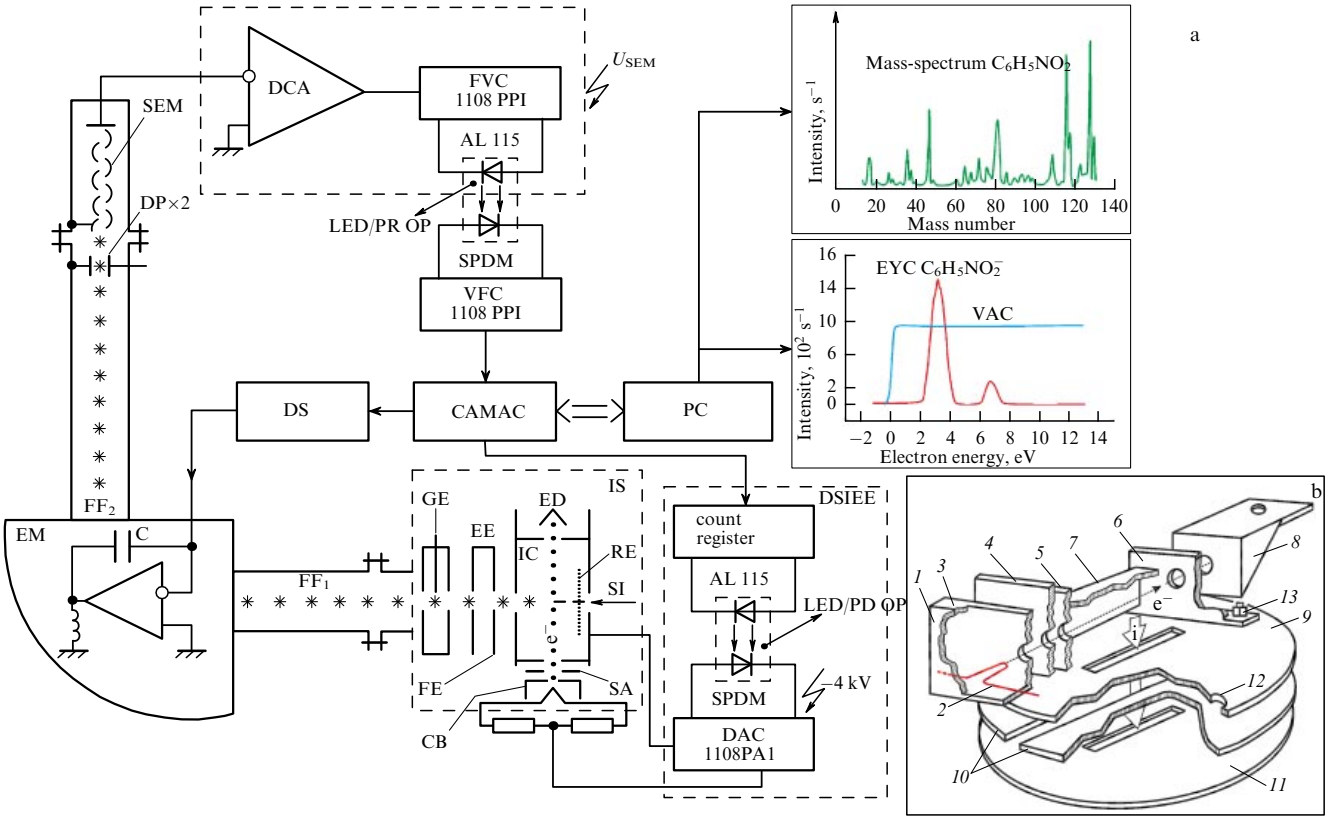

Figure 1. (a) Functional diagram of the mass spectrometer of negative ions based on MI-1201B: FF_1, FF_2 — field-free regions, EM — electromagnet, DP — deflection plates, SEM — secondary electron multiplier MS17/A, DCA — direct current amplifier, VFC/FVC — voltage-frequency converter/frequency-voltage converter, 1108PP1 — product code of the integrated circuit, AL115 — photodiode, LED/PD OP — light emitting diode/photodetector optron pair for high-voltage galvanic isolation, DS — digital sweep unit of the mass-analyzer magnetic field, CAMAC — Computer-Automated Measurement and Control system, PC — personal computer, DSIEE — discrete sweep of ionizing electron energy based on the 1108PA1 digital-to-analog converter (DAC), IS — ion source, SI — substance inflow, CDE — correcting deflection electrode CB — cathode box (*5* in Fig. b), SA — shielding aperture (*4* in Fig. b), IC — ionization chamber (*5*, *6* in Fig. b), RE — repelling electrode) (*7* in Fig. b), ER — electron receiver (*8* in Fig. b), FE — focusing electrode, 1/2 of split electrode (*10* in Fig. b), EE — extracting electrode, 1/2 of split electrode (*10* in Fig. b). (b) Nira-type ion source: *1* — screen (reflector), *2* — directly heated tungsten cathode, *9* — IC cap, *10* — split electrode (1/2 FE, 1/2 EE), *11* — second part of EE, *12* — passageway for the crossarm, *13* — four assembly screws.

from metallic surfaces, the inner surfaces of IS electronic optics (12X18H10T stainless steel: 18% Cr, 10% Ni, 1–1.5% Ti) were coated with a thin layer of soot [52] that prevents gas adsorption on metals [53] and thereby eliminates its influence (stimulatory or suppressive) on their electrical conductivity, depending on gas composition and amount.

3. Classical method for measuring the negative ion lifetime in autodetachment states

In REC processes, negative ions form quasistationary states with a finite lifetime with respect to electron autodetachment. Long-lived ions are recorded by time-of-flight mass-spectrometers if $\tau_a \geqslant 10^{-6}$ s and by static mass-spectrometers if $\tau_a \geqslant 10^{-5}$ s. The fundamental study by Edelson et al. [54] was the first to describe the determination of τ_a under experimental conditions using a time-of-flight mass-spectrometer; the method was developed further by many authors [55]. It was adapted to static mass-spectrometers by V I Khvostenko et al. [56, 57] and presented in greater detail in their later publication [58]. Briefly, N autodetachment ions (the total ion flow) enter the second field-free region (FF_2 in Fig. 1a) at time $t = 0$. This region free of electric and magnetic fields is located between the mass-analyzer and the detection system. During the time t of flight through this region, some ions experience autodetachment of an extra electron and turn into neutral molecules. Here and hereinafter, the number of molecules thus generated, N^0, determines the total neutral component flow. The method for τ_a measurement is based on the extraction of neutral component N^0 from the total flow containing both undecayed ions and the neutral component. The latter is isolated in the electrostatic field of a plane capacitor placed in front of the SEM as a negative potential of 1–1.5 kV is supplied to its plates (DP in Fig. 1). First, the effective yield curve of the total ion flow is recorded as a function of ionizing electron energy with an energy step of $\leqslant 16$ meV; then (after potential supply), the neutral component EYC is written and τ_a is calculated in the online mode on the assumption of exponential decay:

$$N^-(t) = N \exp\left(-\frac{t}{\tau_a}\right), \tag{1}$$

where $N^-(t) = N - N^0$ is the number of undecayed (surviving) ions after time t, and $N^-(t)$ is the negative ion flow.

The above procedure of τ_a measurement in the usual (classical) regime is exemplified in Fig. 2a for SF_6 and in

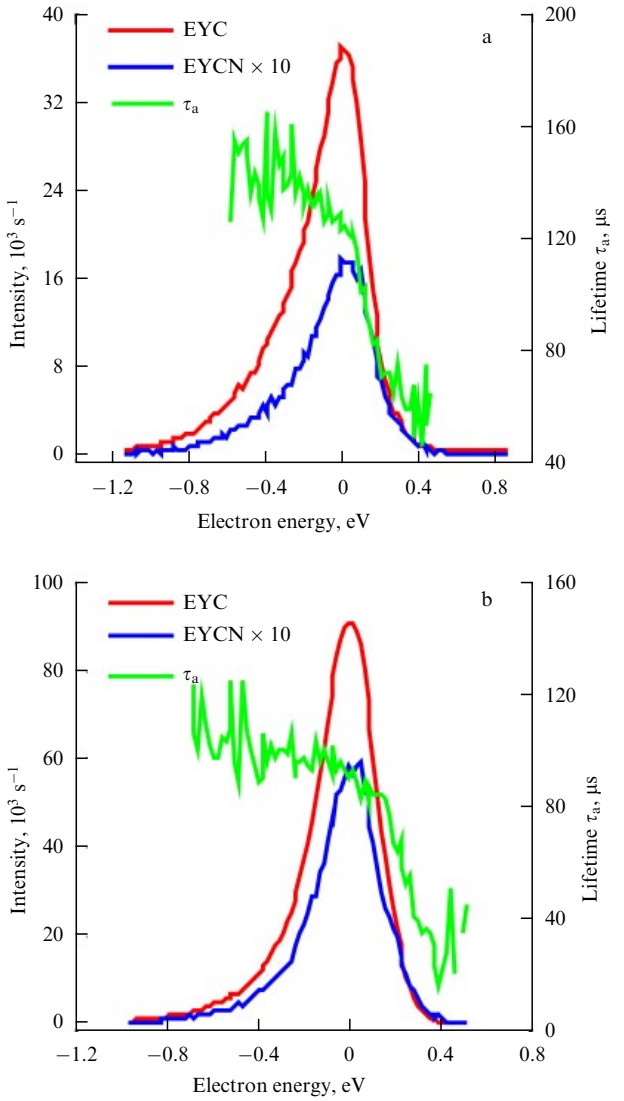

Figure 2. (Color online). Effective yield curves for ions plus neutral component (EYC) and for the neutral component N^0 (EYCN); the autodetachment curve of lifetime τ_a versus ionizing electron energy for SF_6^- (a) and $C_6H_5NO_2^-$ (b) ions.

Fig. 2b for $C_6H_5NO_2$, presenting effective yield curves both for the total flow N (ions plus neutral particles, EYC in Figs 2a, b) and for the neutral component N^0 (EYCN in Figs 2a, b). The same figure presents the 'autodetachment curve' as the dependence of the lifetime of SF_6^- and $C_6H_5NO_2^-$ ions on E_{el} calculated using formula (1). It follows from Fig. 2 that the autodetachment curve exhibits sharp jumps at the ends of the EYC due to a large error of N/N^0 estimation at these ends. Actually, the equality $\tau_a(SF_6^-) = \text{const}$ holds in the maximum intensity region, which reflects the fact that the EYC width is nothing but the electron energy distribution, while the true resonance itself is a δ-function in the sense that SF_6 molecules are well known to uptake only strictly zero-energy electrons.

4. Refined method for measuring the lifetime of negative ions

A new method for measuring τ_a removes from the total ion flow desorbed ions, i.e., those ions that came into contact with the IC surface after formation in the gaseous phase during REC, stabilized there to 'eternal' ions, and eventually returned to the gaseous phase. The method makes use of the substantial difference between the kinetic energies of the desorbed ions and purely gas-phase ions $^aM^-$ in the autoionization state that bypassed the surface. The kinetic energy obtained by the ions from the repelling electrode (RE in Fig. 1a) is $^aM^- \sim 1.5-2.5$ eV and that of desorbed ions is on the order of k_BT, therefore, even at $T_{IC} = 300$ °C (which is practically unattainable in an IC) it does not exceed 0.03 eV [59, 60]. It is this difference between the kinetic energies that allowed the separation of two types of ions in our experiments with the use of an ion filter designed for a modified ion source.

The ion filter was made by replacing the split electrode of the IS ion-optical system (FE, EE in Fig. 1a; *10* in Fig. 1b) with a new electrode of the same design and material as those of the IC cap. The 2 × 8-mm slit in the new electrode was covered with a fine-structured metallic mesh from a secondary electron multiplier (SEM-2A) lacking magnetic properties and having fairly good transparency (~ 80%), as shown by A M Tyutikov in Ref. [61]. The filter, having a negative potential of ~ 1 V and placed in the path of ions escaping the IC, constitutes an obstacle for the desorbed ions due to their low kinetic energy (a few hundredths of an electron volt) and transmits only high-energy gas-phase $^aM^-$.

A similar method is used to measure mean effective cross section Q_a of the electron capture process (the electron filter method proposed by Loeb, Lusk, and Cravath [62, 63]) in Ref. [64]. The filter is a metallic grid of fine wires, between which a high-frequency alternating electric field can be applied. Given the adequate choice of the field strength, all electrons of the beam reaching the filter can be deflected by one wire or another, whereas relatively heavy negative ions are practically unaffected by the field. For this reason, the measurement of the electron component of beam current in front of the filter reduces to determining the degree of beam current decrease after its passage through the filter. V N Ageev and E N Kutsenko removed an undesirable component from the total particle flow using fine-structured copper grid to separate charged and uncharged desorption products emitted from the cathode surface of a pulsed time-of-flight mass-spectrometer bombarded by slow electrons when ions were detained by the potential difference between the adsorbent and one of the IS grids [65]. It should be emphasized that the replacement of the split electrode intended to focus the ion beam leaving the IC with a new electrode in the present study caused no appreciable decrease in intensity, because the ion beam was focused in the modified construction by ions themselves adsorbed on the IC cap (as most vulnerable to adsorption among all other IC surfaces) and by the potential supplied to the correcting deflection electrode [66]. There is reason to think that the presence of the grid enhances focusing by ions adsorbed on the IC cap, because the stopping potential of the grid increases the number of negative ions on it.

It was mentioned above that a potential negative with respect to the IC cap, i.e., cutoff voltage U_{cut}, was applied to the ion filter for separating ions of two types. To determine the exact U_{cut} value, each experiment was started from the tuning to the peak signal coming to an SEM, with the subsequent voltage application to the deflection plates (DP in Fig. 1) placed in front of the SEM. As a result, the multiplier recorded only neutral particles N^0 (i.e., the neutral

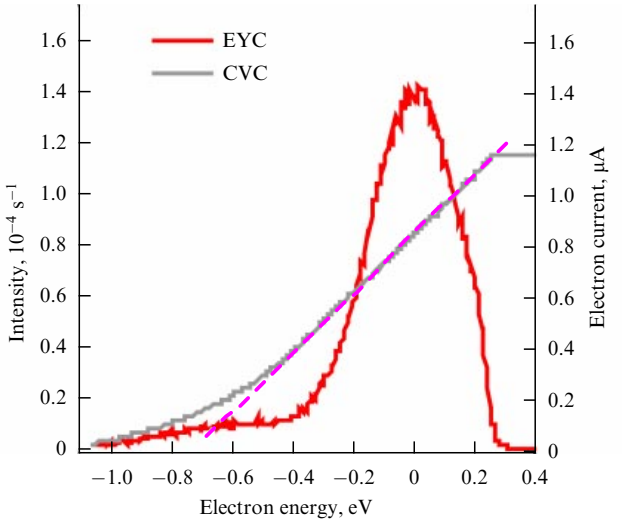

Figure 3. (Color online.) Effective yield curve for SF_6 ions. Real CVC and the linear region of ascending CVC portion (dashed line) of the ion source.

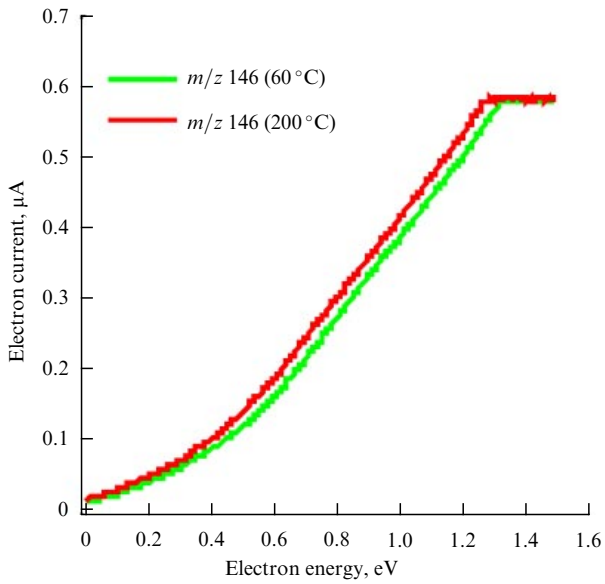

Figure 4. (Color online.) Current-voltage characteristic of ionizing electron energy in the record of SF_6 ion EYC at $T_{IC} = 60$ (green curve) and $T_{IC} = 200\,°C$ (red curve).

component of the total flow of N ions), which is the usual procedure in the τ_a measurements described above. The intensity of the neutral component $I(N^0)$ was fixed to be used further as a reference to evaluate the contribution of purely gas-phase $^aM^-$ to the total flow, taking into consideration that the neutral component (FF_2 region) arises only from these $^aM^-$ ions. Then, voltage was removed from the deflection plates, and the full signal (ions plus neutral particles) arrived at the SEM again, after which voltage U_{cut} was applied to the grid such that the total signal was reduced to $I(N^0)$. This operation removed all desorbed ions from the beam. Voltage U_{cut} was chosen separately for each individual experiment, even though it has a characteristic value $U_{cut} \approx -1 \pm 0.25$ V. After this preliminary procedure, the instrument could be used to measure τ_a by the new method.

Modifying the ion source necessitated checking the compliance of its adjustment with required standards. Specifically, the EYC was recorded on the linear region of the ascending portion of the current-voltage characteristic (CVC) (dashed line in Fig. 3). Also, the direct current amplifier (DCA in Fig. 1a) was replaced by a pulsed broadband amplifier with a linear counter characteristic up to 10^6 s^{-1}. Therefore, the N and N^0 values needed to calculate τ_a were measured by direct pulse counting in the framework of the refined method.

An important part of our work was the elucidation of the temperature dependence of τ_a with the use of an ion filter. This dependence was derived for $\tau_a(SF_6^-)$ and $\tau_a(C_6H_5NO_2^-)$ ions in a range from $T_{IC} = 60$ to $T_{IC} = 200\,°C$ at $E_{el} \sim 0$ eV, where ions were generated via the vibrationally excited Feshbach resonance mechanism [67]. To this effect, the EYC of the total flow (ions plus neutral particles) and the curve of the effective yield of the neutral component N^0 (EYCN) were recorded. The EYC were recorded in the said range with a $(20.0 \pm 0.5)\,°C$ temperature step and 4-meV quantization of, ionizing electron energy. Each next record was made 5 min after setting the temperature of the preceding sample. Temperature dependences of $\tau_a(SF_6^-)$ and $\tau_a(C_6H_5NO_2^-)$ were interpreted with reference to the τ_a value corresponding to the EYC maximum. The conditions of single collisions in the IC were evaluated from the ratio of IC linear dimensions ($l \approx 1$ cm) to the mean free path of gas molecules λ calculated using the formula [68]

$$\lambda = 10^{-5}\left(\frac{t}{273}\right)\left(\frac{760}{p}\right) \quad [\text{cm}]\,, \tag{2}$$

where t is Celsius temperature and p is pressure in mm Hg (Torr).

When the pressure in the IC at $T_{IC} = 200\,°C$ was $p \leqslant 10^{-5}$ mm Hg, $\lambda \sim 0.6 \times 10^3$ cm. Thus, it follows from the ratio of linear dimensions that the probability of ion collision with the residual gas in the IC was $< 0.2\%$ of the probability of collisions of all ions. The value of 0.2% qualitatively agrees with the result of V L Tal'roze and E L Frankevich [59], who experimentally confirmed that at pressures $\sim 10^{-4}$ mm Hg only a minor part of primary ions reacts with molecules of the residual gas, so that neglecting this value does not introduce essential error.

To recall, redesigning the IC (replacement of the split electrode) had no appreciable effect on its CVC. Variants of the CVC written at different temperatures are presented in Fig. 4. A minor increase in CVC current associated with a rise in IC temperature did not cause distortion of $\tau_a(^aM^-)$ measurements in the linear region of the ascending CVC portion.

The materials under study were introduced into the IC through the metering valve of the inlet 'comb' of the commercial instrument.

5. Measurement of the lifetime of sulfur hexafluoride and nitrobenzene negative ions by the refined method. Temperature dependence

New data on the lifetimes of negative molecular ions $\tau_a(SF_6^-)$ and $\tau_a(C_6H_5NO_2^-)$ obtained by the refined method with the use of the ion filter are presented in Figs 5 and 6.

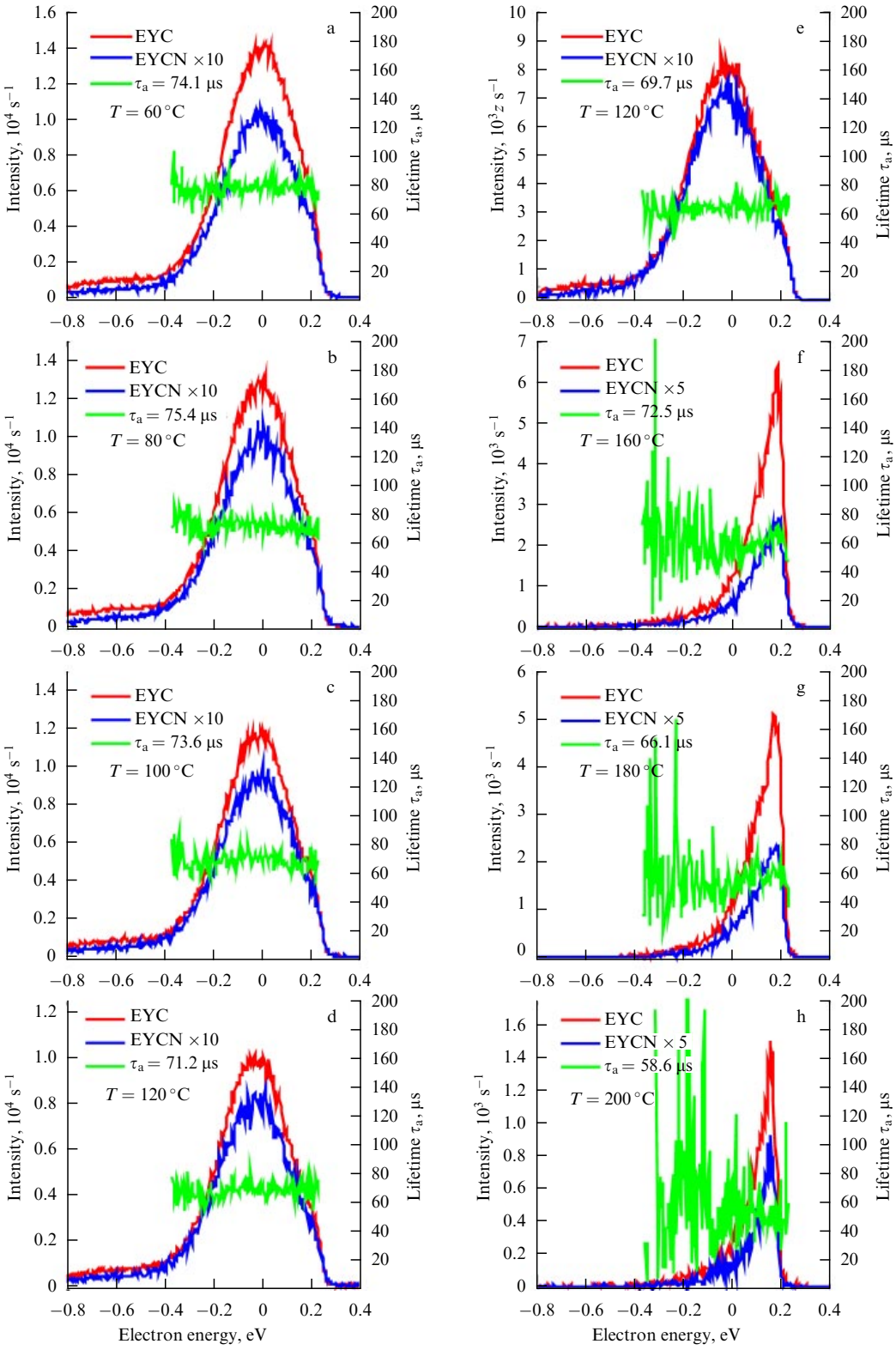

Figure 5. (Color online.) Effective yield curves for the total flow N (SF_6 ions plus neutral component, EYC) and SF_6^0 neutral component (EYCN); the autodetachment curve of lifetime τ_a recorded at various temperatures of the ionization chamber with the use of an ion filter.

It follows from SF_6 and $C_6H_5NO_2$ studies that newly measured τ_a are smaller than routinely obtained values. Furthermore, they remain within statistical straggling in the temperature range from $T_{IC} = 60$ to $T_{IC} = 160\,°C$. For example, $\tau_a(SF_6^-)$ indicates that the scatter of lifetime measurements comes from ion adsorption on the IC surface rather than from multiexponentiality.

At the same time, some peculiarities of experimental findings were observed largely at $T_{IC} > 160°$, e.g., a change in the EYC shape and a slight decrease in $\tau_a(SF_6^-)$ (from 77.5 to 58.7 μs) and $\tau_a(C_6H_5NO_2^-)$ (from 54 to 43 μs). These peculiarities arise from the ability of negative ions (SF_6^-, $C_6H_5NO_2^-$) to adsorb on the IC walls and the influence of their number on the number of gas-

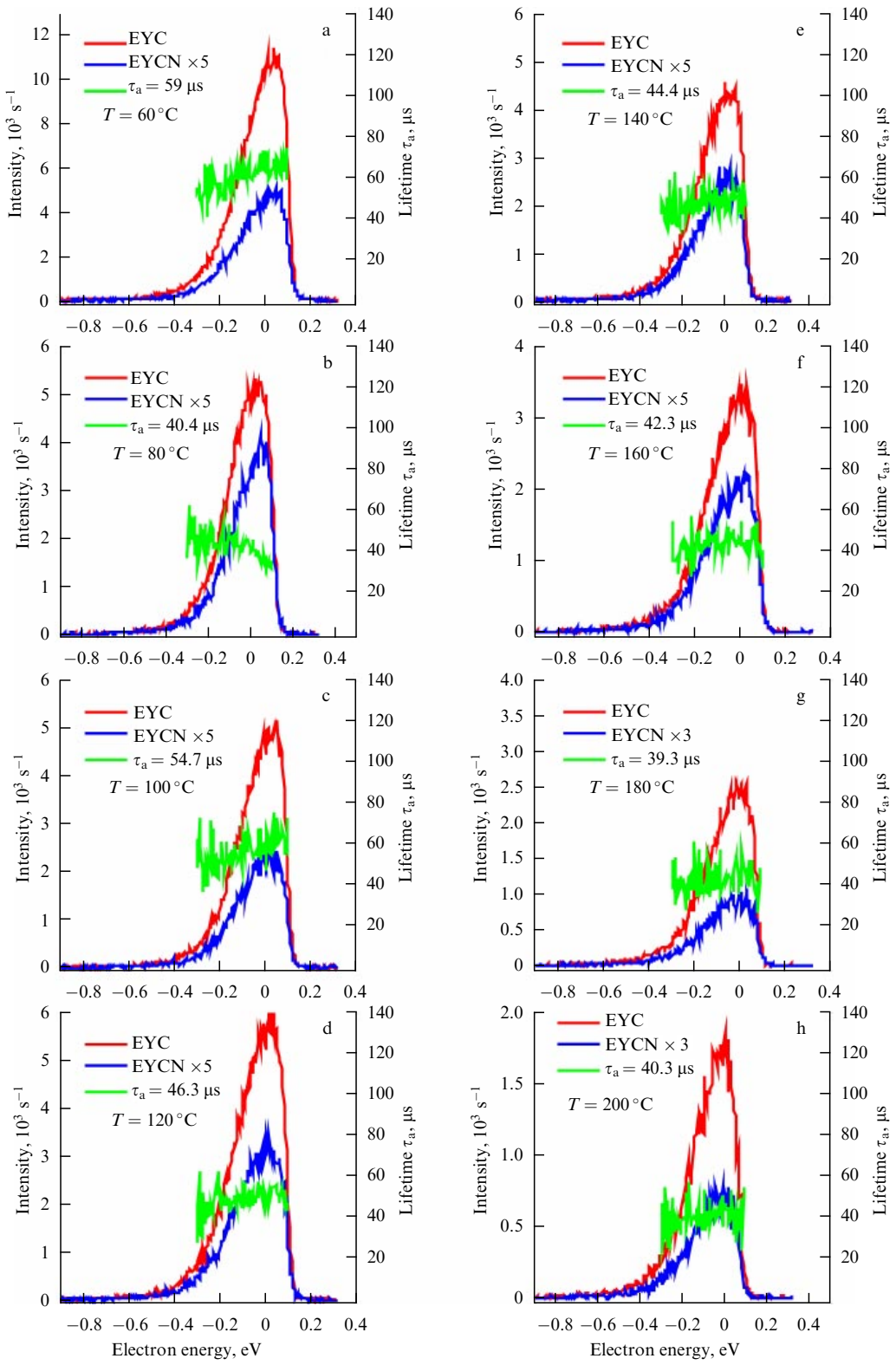

Figure 6. (Color online.) Effective yield curves for $C_6H_5NO_2$ ions (EYC) and $C_6H_5NO_2^0$ neutral component (EYCN); the autodetachment curves of mean lifetime τ_a dependence recorded at various temperatures of the ionization chamber with the use of an ion filter.

phase ions reaching the detection system and directly measured by the refined method proposed in this article. Massive adsorption suppresses intensity of the purely gas-phase ion current and reduces the registered intensities, which increases measurement errors. Some characteristic features of such adsorption are discussed in Section 6.

6. Influence of adsorption on the dynamics of purely gas-phase ions detected by the refined method

When temperature T_{IC} amounts to 160 °C, for SF_6^- ions the well apparent shift of ionizing electron energy maxima on the

EYC is observed. Hickam and Berg showed in a study dating back to 1959 [69] that a change in temperature of an ion source can cause serious changes on a negative ion EYC for certain gases. However, the authors of [69] emphasized that the observed reduction in the SF_6^- EYC amplitude is much greater than that attributable to altered gas density. They observed practically no changes in the curve shape, except a marked shift along the electron energy axis. Similar results were obtained in all our studies (Fig. 5a–e) with the exception of the shift of the maximum along the ionizing electron energy axis in the present work. This suggests the absence of an appreciable distortion of the ionizing electron energy distribution with a change in temperature (see Fig. 4). However, any change in adsorbent temperature alters the pressure and therefore the ratio of free to adsorbed negative ions, meaning that a shift may result either in a reduced shielding thickness or in an enlarged area free from adsorbed molecules. F F Vol'kenshtein showed in [70] that the former result has a direct bearing on the shell thickness (the layer of adsorbed molecules) that can be varied to control the adsorption capacity, catalytic activity, and selectivity of the sample. Importantly, the shell thickness L must be smaller than the shielding length ($L < 10^{-4} - 10^{-5}$ cm), but not too thin to be considered a separate phase ($L \geqslant 10^{-6}$ cm). For example, "only two ethylene ($CH_2 = CH_2$) monolayers are needed to shield argon molecules from the field of the graphitized carbon black surface; isosteric heat of argon adsorption remains practically unaltered as preliminary adsorption of $CH_2 = CH_2$ continues to grow" [71]. The second reason is consistent with Becker's measurements for atoms [72] suggesting that the "evaporation heat of atoms decreases with increasing θ whereas evaporation heat of ions grows with θ (θ is a part of the surface covered by adatoms)" [73]. Any of the conjectured options is promoted by fast ion neutralization on the IC surface; therefore, the thermodynamic adsorption-neutralization-desorption equilibrium is reached at a larger number of adsorbed ions on the surface, which affects ion EYC intensity, especially at $T_{IC} \geqslant 160\,^{\circ}C$.

Faster ion neutralization on the IC surface in a temperature range from $T_{IC} = 160$ to $T_{IC} = 200\,^{\circ}C$ is also suggested by the altered shape of ion and neutral component EYCs, an effect previously unencountered in our practice. In terms of the classification by S Brunauer, L S Deming, W S Deming, and E Teller [74], the curves in Figs 5f–h can be regarded as type III adsorption isotherms [75]. Isotherms of this type with a characteristic shape concave with respect to the abscissa axis describe processes on a surface with a relatively weak adsorptive capacity; they manifest themselves in adsorption on nonporous and macroporous solid objects (in our case, stainless steel coated with soot, i.e., practically spherical particles — combustion products of plexiglass (organic glass)). Only soot specially nonoxidized by heating in the air or oxygen or by treatment with liquid oxidizers is nonporous, although if it has a rough surface [76]. Soot particles arrayed in chains form a loose spatial structure [77] that appears to adsorb air components in the course of NI open fuming. Consequently, the exclusion of injection of desorbed 'eternal' ions from the ion beam being registered confirms the weak adsorbability of SF_6 molecules in the said temperature range, which accounts for the increased probability of ion neutralization on the IC surface.

Comparing SF_6^- and $C_6H_5NO_2^-$ EYCs (see Figs 5, 6) allows us to relate the observed experimental fact of the absence of changes in their shape at $T_{IC} \geqslant 160\,^{\circ}C$ to a higher accommodation coefficient of $C_6H_5NO_2$ molecules characterizing the fraction of gas particles hitting the surface which are adsorbed on it. It was demonstrated in [76] that the degree of removal of physically adsorbed molecules from the surface at a given vacuum level depends on the nature of these molecules, chemical properties of the surface, temperature, evacuation time, pore structure, amount of adsorbent, and characteristics of the equipment. The influence of the nature of molecules and surface migration [78, 79] was confirmed by N V Cherepnin [80], who undertook a comparative analysis of adsorption process energies based on the literature data. The analysis showed that the binding energy of physically adsorbed particles depends on their size: as a rule, the bigger the particle, the higher the binding energy. This suggests a similarity between the processes of physical adsorption and liquid vapor condensation, i.e., the higher the molecular weight of a liquid, the higher its boiling temperature. As a consequence, the process of adsorption becomes increasingly irreversible with temperature that grows parallel to the strengthening of the adhesion of specifically adsorbed anions to the IC surface. It enhances the probability of ion neutralization on the surface and means that the energy liberated during physical adsorption may characterize the strength of the adhesion between the particles and the adsorbent.

A weak inverse correlation between τ_a and temperature (Figs 7, 8) within the decreasing range from 74 μs to $\tau_a = 58.7$ μs for $\tau_a(SF_6^-)$ and from 59 μs to 43 μs for $\tau_a(C_6H_5NO_2^-)$ is due to the dynamic process on the IC surface that manifests itself especially in the registration of neutral particles (ions that lose the extra electron through autodetachment) on the SEM anode resistor at IC temperature $T_{IC} \geqslant 180\,^{\circ}C$, because negative ions extract more electrons than analogous positive ones [81, 82] (neutral atoms pull out approximately as many secondary electrons as singly charged positive ions having the same energy [83, 84]) [85].

Enhancement of the voltage drop on the anode resistor of the SEM during the detection of short pulses is inefficient, because the signal intensity amplitude at the exit from the multiplier $U_{out} = kI_{in}R_a$ is limited by the maximum allowable size of the anode resistor $R_a = \tau_p/C_a$, where k is the amplifier coefficient, I_{in} is the input current of the SEM anode, τ_p is pulse duration, and C_a is the capacity of SEM anode and amplifier input circuit. The inclusion of the pulsed broadband amplifier with low input resistance and a transformation coefficient of 40 mV μA^{-1} [86] in accordance with the direct input current/output voltage conversion scheme would allow improving the sensitivity of the measuring system in a broad range of received frequencies. However, such a conversion requires rearrangement of the SEM connection circuit [87] (negative voltage applied to the SEM cathode and anode grounding), which is likely to result in recording charged and neutral particles with different efficiency (unequal sensitivity of the SEM to charged (k_1) and neutral (k_2) particles, where $k_1 \neq k_2$ are SEM secondary emission coefficients). On the other hand, the IC temperature appears to influence the ion EYC and EYCN that are written in two steps and serve as a basis for calculating τ_a. It follows from Figs 5, 6 that EYC noise in the ionizing electron energy range from −0.4 to 0.4 eV is higher than the zero (out-of-range) line noise. At the same time, the counting rate of SEM noise pulses is 3–5 s^{-1} if the amplifier cathode is grounded (Fig. 1a) and positive voltage is applied to the anode [87], which suggests

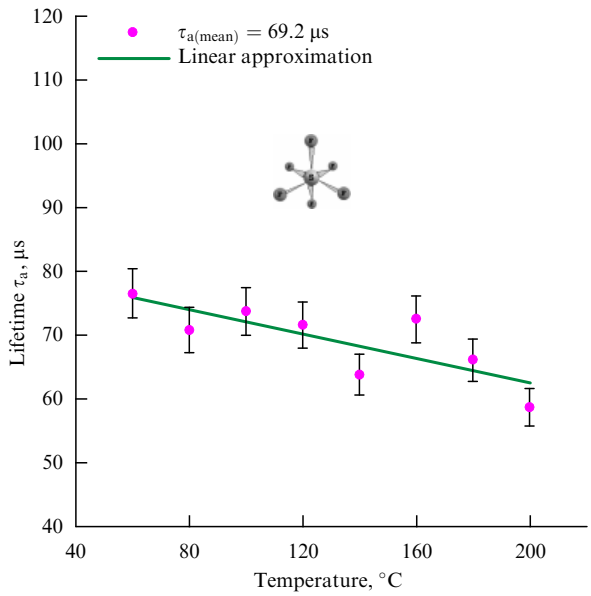

Figure 7. Scatter diagram and correlation relationship of the dependence of SF_6^- mean lifetime τ_a on ionization chamber temperature.

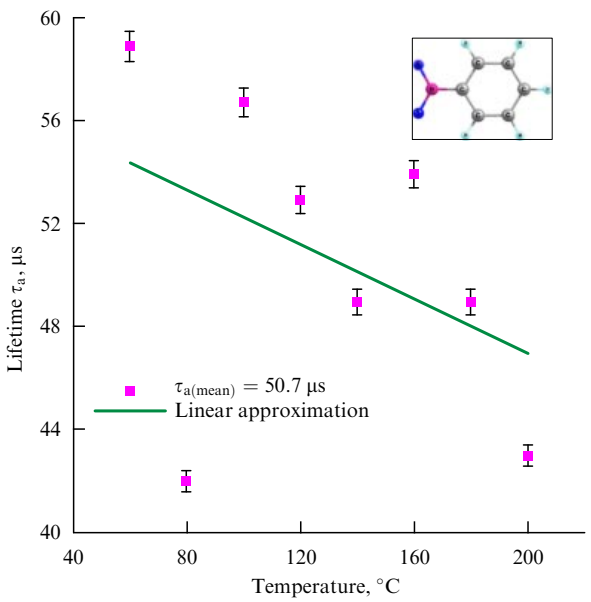

Figure 8. Scatter diagram and correlation relationship of the dependence of $C_6H_5NO_2^-$ mean lifetime τ_a on ionization chamber temperature.

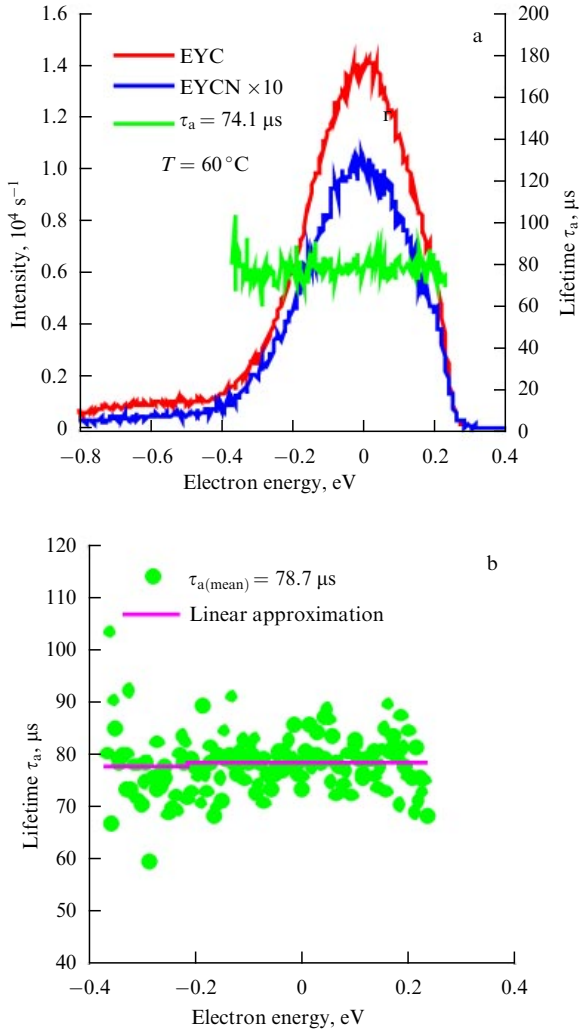

Figure 9. (Color online). (a) Effective yield curves for SF_6^- ions together with neutral particles (EYC) and for the neutral component N^0 (EYCN); the autodetachment curve of the lifetime τ_a versus ionizing electron energy. (b) Scatter diagram and linear correlation between ion lifetime and ionizing electron energy.

that EYC noise in the above range is a function of the primary current and input circuit discrimination threshold of the pulsed amplifier which accounts for spikes $\sim 10\%$ in the τ_a scatter diagram for SF_6^- ions presented as an example in Fig. 9. Scatter of τ_a is due to statistical noises resembling shot noise[1] inherent in low currents, such as those in vacuum tubes. This noise originates from probability processes related to IC adsorbing surface inhomogeneity. According to N V Cherepnin [80], "the adsorbent surface contains adsorption centres differing in attractive forces and the respective binding energies. Therefore, by referring the binding energy to a mole of the adsorbed gas we express the mean adsorption energy for 6×10^{23} gas molecules including those with the binding energy either higher or lower than its mean value; in other words, molecules are adsorbed irregularly over the adsorbent surface." All this is known to greatly affect the character of charged particle emission, making particle desorption equally irregular.

The strong negative correlation of SF_6^- and $C_6H_5NO_2^-$ signal intensities with temperature (Figs 10, 11) also arises from the variation of adsorbability of the IC surface. The adsorption capacity of a surface usually manifests itself as a change in pressure in the adsorption volume. Experiments by N A Balashova and N S Merkulova [88], as well as basic research based on the general provisions of the electron theory of chemisorption and catalysis developed by F F Vol'kenshtein and Sh M Kogan [89], give evidence that physically adsorbed gas particles are readily 'evaporated' from a surface under UV, visible, and infrared irradiation. This means that a change in adsorbent temperature as a form of irradiation alters both pressure and the free-to-adsorbed

[1] Shot noise is defined as the random fluctuation of currents and voltages around the mean value in the circuits of electric and electronic devices owing to the discrete nature of electric charge carriers, such as electrons and ions.

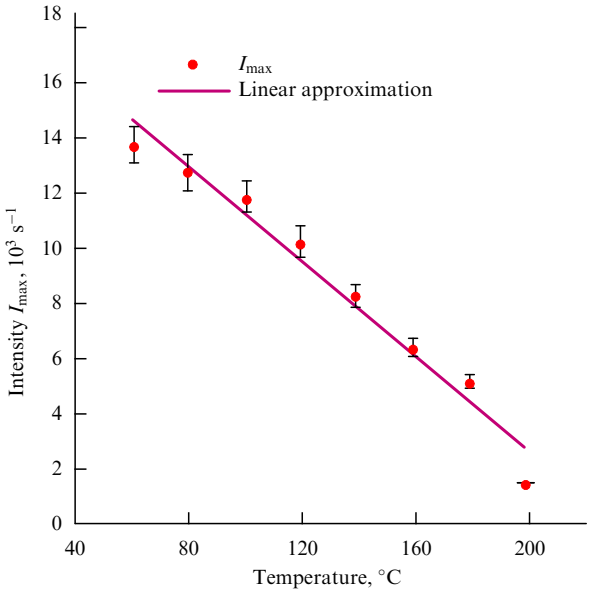

Figure 10. Scatter diagram and correlation relationship of the dependence of SF_6^- intensity on ionization chamber temperature.

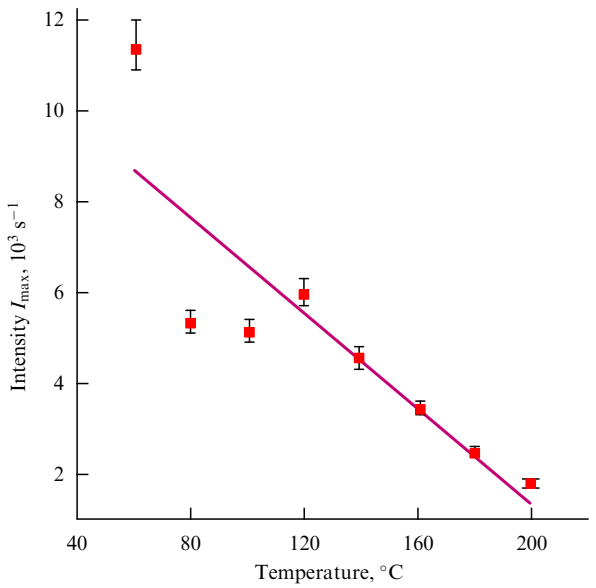

Figure 11. Scatter diagram and correlation relationship of the dependence of $C_6H_5NO_2^-$ intensity on ionization chamber temperature. I_{max} — signal intensity at the peak of the effective yield curve (see Figs 5, 6).

gas ratio. It cleans the IC surface and facilitates neutralization of SF_6^- and $C_6H_5NO_2^-$ ions which manifest themselves as a drop in signal intensity. The observed linear dependence of SF_6^- and $C_6H_5NO_2^-$ signal intensities on IC temperature confirms the absence of secondary processes (e.g., surface ionization on the thermocathode).

7. Conclusion

The present work was designed to investigate resonant electron capture (REC) by sulfur hexafluoride and nitrobenzene molecules using an MI-1201B static mass-spectrometer with a 90 sector magnetic field modified for the detection of negative ions in the pulse counting mode. The study was carried out by the refined method based on the use of a specially constructed ion filter placed in the ion source. The filter excluded those ions from the total ion flow directed to the detection system that came into contact with the IC surface after formation in the gaseous phase during REC, stabilized there, and partly desorbed thereafter to join purely gas-phase autodetachment ions, the main subjects of our interest. Lifetimes τ_a of negative molecular ions of both compounds were measured in the conventional regime (without IC heating) and in a wide temperature range from 60 to 200 °C. The measured τ_a values were $\approx (69.20 \pm 0.05)$ μs for SF_6^- ions and $\approx (50.70 \pm 0.05)$ μs for $C_6H_5NO_2^-$, i.e., half the typical values for instruments of this class at the IC nominal temperature $T_{IC} = 60$ °C. Deviation of τ_a from the arithmetic mean at the autodetachment curve inside resonance amounted to ± 10 μs. The value $\tau_a \pm 10$ μs originates from the probability process of SF_6^- and $C_6H_5NO_2^-$ adsorption on the IC surface, because such adsorption influences gas-phase ion intensity, and from the separate recording of the total flow and neutral component flow EYCs. Taken together, these factors affect measurement accuracy. At the same time, the rather weak negative correlation between τ_a and temperature allows the conclusion that τ_a does not depend on temperature.

To conclude, the present study showed that in the case of removal of desorbed ions from the total flow the measured τ_a values are virtually independent of IC temperature and therefore of the temperature of initial molecules giving rise to negative ions during REC. This finding brings into question the generally accepted 'multiexponentiality' concept usually employed to account for the scatter of experimental τ_a values, because this concept implies such a dependence (the higher the temperature, the shorter τ_a).

In summary, the refined method proposed in the present work to improve the experimental assessment of the lifetime of long-lived negative ions allows minimizing experimental errors caused by effects of ion interaction with the IC surface and thereby obtaining lifetime measurements closest to the true value. This approach yields precise theoretical estimates for a better understanding of the mechanisms behind ion formation and decay and for the practical application of materials with the properties of strong electron acceptors widely used in many modern technologies.

References

1. Feshbach H *Ann. Physics* **5** 357 (1958)
2. Fano U *Phys. Rev.* **124** 1866 (1961)
3. Demkov Yu N *Sov. Phys. JETP* **22** 615 (1965); *Zh. Eksp. Teor. Fiz.* **49** 885 (1965)
4. O'Malley T F *Phys. Rev.* **150** 14 (1966)
5. Bardsley J N, Mandl F *Rep. Prog. Phys.* **31** 471 (1968)
6. Herzenberg A *J. Chem. Phys.* **51** 4942 (1969)
7. Taylor H S, Thomas L D *Phys. Rev. Lett.* **28** 1091 (1972)
8. Schulz G J *Rev. Mod. Phys.* **45** 423 (1973)
9. Khvostenko V I, Tolstikov G A *Russ. Chem. Rev.* **45** 127 (1976); *Usp. Khim.* **45** 251 (1976)
10. Christophorou L G, in *Advances in Electronics and Electron Physics* Vol. 46 (Ed. L Marton) (New York: Academic Press, 1978) p. 55
11. Smirnov B M *Negative Ions* (New York: McGraw-Hill, 1982); Translated from Russian: *Otritsatel'nye Iony* (Moscow: Atomizdat, 1978)
12. Illenberger E, Smirnov B M *Phys. Usp.* **41** 651 (1998); *Usp. Fiz. Nauk* **168** 731 (1998)
13. Simons J *Annu. Rev. Phys. Chem.* **62** 107 (2011)
14. Fabrikant I I *Phys. Rev. A* **94** 052707 (2016)
15. Zawadzki M et al. *Phys. Rev. Lett.* **121** 143402 (2018)

16. Buchel'nikova N S *Usp. Fiz. Nauk* **65** 351 (1958)
17. Aleksandrov N L, Napartovich A P *Phys. Usp.* **36** 107 (1993); *Usp. Fiz. Nauk* **163** (3) 1 (1993)
18. Checchetto V et al. *Biophys. Chem.* **182** 51 (2013)
19. Brooks J S *Chem. Soc. Rev.* **39** 2667 (2010)
20. Koh W et al. *ChemPhysChem.* **17** 1095 (2016)
21. Khvostenko V I, Vorob'yov A S, Khvostenko O G *J. Phys. B* **23** 1975 (1990)
22. Khvostenko O G et al. *J. Electron Spectrosc. Relat. Phenom.* **199** 1 (2015)
23. Blau L M, Novick R, Weinflash D *Phys. Rev. Lett.* **24** 2168 (1970)
24. Khvostenko O G, Tuimedov G M *Rapid Commun. Mass Spectrom.* **20** 3699 (2006)
25. Khvostenko O G et al. *Chem. Phys. Lett.* **711** 81 (2018)
26. Edelson D, Grifiths J E, McAffe K B (Jr) *J. Chem. Phys.* **37** 917 (1962)
27. Liu Y, Suess L, Dunning F B *J. Chem. Phys.* **122** 214313 (2005)
28. Rajput J, Lammich L, Andersen L H *J. Phys. Rev. Lett.* **100** 153001 (2008)
29. Menk S, Dissertation (Germany, 2013)
30. Harland P W, Thynne J C J *Inorg. Nucl. Chem. Lett.* **7** 29 (1971)
31. Stock M G *Dyn. Mass Spectrom.* **4** 197 (1976)
32. Odom P W, Smith D L, Futrell J H *J. Phys. B* **8** 1349 (1975)
33. Compton R N et al. *J. Chem. Phys.* **45** 4634 (1966)
34. Lukin V G, Tuimedov G M *Instrum. Exp. Tech.* **56** 565 (2013); *Prib. Tekh. Eksp.* (5) 77 (2013)
35. Harland P W, Thynne J C J *J. Phys. Chem.* **75** 3517 (1971)
36. Klots C F *J. Chem. Phys.* **46** 1197 (1967)
37. Vorob'ev A S et al. *Tech. Phys.* **54** 1255 (2009); *Zh. Tekh. Fiz.* **79** (9) 11 (2009)
38. Lukin V G, Khvostenko O G, Tuimedov G M *Int. J. Mass Spectrom.* **399 – 400** 17 (2016)
39. Lukin V G, Khvostenko O G, Tuimedov G M *Tech. Phys. Lett.* **42** 215 (2016); *Pis'ma Zh. Eksp. Teor. Fiz.* **42** (4) 96 (2016)
40. Lukin V G, Khvostenko O G, Tuimedov G M *Tech. Phys.* **62** 998 (2017); *Zh. Tekh. Fiz.* **87** 982 (2017)
41. Lukin V G, Khvostenko O G *Phys. Usp.* **60** 911 (2017); *Usp. Fiz. Nauk* **187** 981 (2017)
42. Lukin V G, Tuimedov G M *Instrum. Exp. Tech.* **62** 47 (2019); *Prib. Tekh. Eksp.* (1) 51 (2019)
43. Kaminsky M *Atomic and Ionic Impact Phenomena on Metal Surfaces* (Berlin: Springer-Verlag, 1965); Translated into Russian: *Atomnye i Ionnye Stolknoveniya na Poverkhnosti Metalla* (Moscow: Mir, 1967)
44. Smirnov B M *Physics of Atoms and Ions* (New York: Springer, 2003); Translated from Russian: *Fizika Atoma i Iona* (Moscow: Energoatomizdat, 1986)
45. Masel R I *Principles of Adsorption and Reaction on Solid Surfaces* (New York: Wiley, 1996)
46. MacDonald R J, O'Connor D J *Aust. J. Phys.* **37** 389 (1984)
47. Cooper B H et al. *Nucl. Instrum. Meth. Phys. Res. B* **64** 49 (1992)
48. Kammerer J, Carle R, Kammerer D R *J. Agric. Food Chem.* **59** 22 (2011)
49. Gupta S et al. *AIP Adv.* **8** 065225 (2018)
50. Minissale M, Congiu E, Dulieu F *Astron. Astrophys.* **585** A146 (2016)
51. Filatov V N, Sysoev A A, Morozov O V *Prib. Tekh. Eksp.* (1) 77 (1981)
52. Roberts T D, Burch B D *Rev. Sci. Insrum.* **35** 1067 (1964); *Prib. Nauch. Issled.* (8) 140 (1964)
53. Cherepnin N V *Vakuumnye Svoistva Materialov dlya Elektronnykh Priborov* (Vacuum Properties of Materials for Electronic Devices) (Moscow: Sovetskoe Radio, 1966)
54. Edelson D, Griffiths J E, McAfee K B (Jr.) *J. Chem. Phys.* **37** 917 (1962)
55. Hadjiantjniou A, Christophorou L G, Carter J G *J. Chem. Soc. Faraday Trans. 2* **69** 1691 (1973)
56. Khvostenko V I *Mass-Spektrometriya Otritsatel'nykh Ionov v Organicheskoi Khimii* (Mass-Spectrometry of Negative Ions in Organic Chemistry) (Moscow: Nauka, 1981)
57. Khvostenko V I et al. *Izv. Akad. Nauk SSSR. Ser. Khim.* (3) 681 (1973)
58. Lukin V G, Vorob'ev A S, Lomakin G S *Instrum. Exp. Tech.* **52** 560 (2009); *Prib. Tekh. Eksp.* (4) 121 (2009)
59. Tal'roze V L, Rankevich E L *Zh. Fiz. Khim.* **34** 2709 (1960)
60. Giese C F "Ion-neutral reactions", in *Advances in Chemical Physics: Molecular Beams* Vol. 10 (Ed. J Rose) (New York: John Wiley and Sons, 1966) p. 247; Translated into Russian: "Reaktsii ionov s neitral'nymi chastitsami", in *Issledovaniya s Molekulyarnymi Puchkami* (Eds A M Brodskii, V B Leonas) (Moscow: Mir, 1969)
61. Tyutikov A M *Sov. Phys. Usp.* **13** 204 (1970); *Usp. Fiz. Nauk* **100** 467 (1970)
62. Cravath A M *Phys. Rev.* **33** 605 (1929)
63. Loeb L B *Phys. Rev.* **48** 684 (1935)
64. Massey H S W, Burhop E H S *Electronic and Ionic Impact Phenomena* (Oxford: Clarendon Press, 1952); Translated into Russian: *Elektronnye i Ionnye Stolknoveniya* (Moscow: IL, 1958)
65. Ageev V N, Kutsenko E N *Zh. Tekh. Fiz.* **39** 1275 (1969)
66. *Tekhnicheskoe Opisanie i Instruktsiya po Ekspluatatsii Mass-spektrometra MI-1201B* (MI-1201B Mass-Spectrometer: Technical Description and Operation Manual) (Sumy: Proizvodstvennoe Ob'edinenie 'Elektron', 1983)
67. Christophorou L G *Atomic and Molecular Radiation Physics* (London: Willey-Interscience, 1971)
68. De Boer J H *The Dynamical Character of Adsorption* (Oxford: Clarendon P, 1968); Translated into Russian: *Dinamicheskii Kharakter Adsorbtsii* (Moscow: IL, 1962)
69. Hickam W M, Berg D, in *Advances in Mass Spectrometry* (Ed. J D Waldron) (New York: Pergamon Press, 1959) p. 458; Translated into Russian: *Uspekhi Mass-Spektrometrii* (Ed. J D Waldron) (Moscow: IL, 1963)
70. Vol'kenshtein F F *Fizikokhimiya Poverkhnosti Poluprovodnikov* (Physical Chemistry of Superconductor Surface) (Moscow: Nauka, 1973)
71. Adamson A W *Physical Chemistry of Surfaces* (New York: Academic Press, 1973); Translated into Russian *Fizicheskaya Khimiya Poverkhnostei* (Moscow: Mir, 1979)
72. Becker J A *Phys. Rev.* **28** 341 (1926)
73. De Boer J H *Electron Emission and Adsorption Phenomena* (Cambridge: The Univ. Press, 1935); Translated into Russian: *Elektronnaya Emissiya i Yavleniya Adsorbtsii* (Moscow–Leningrad: GROTL, 1936)
74. Brunaauer S et al. *J. Am. Chem. Soc.* **62** 1723 (1940)
75. Gregg S J, Sing K S W *Adsorption, Surface Area and Porosity* (London: Academic Press, 1982); Translated into Russian: *Adsorbtsiya. Udel'naya Poverkhnost'. Poristost'* (Moscow: Mir, 1984)
76. Avgul' N N, Kiselev A V, Poshkus D P *Adsorbtsiya Gazov i Parov na Odnorodnykh Poverkhnostyakh* (Adsorption of Gazes and Vapours at the Homogeneous Surfaces) (Moscow: Khimiya, 1975)
77. Karnaukhov A P, in *Adsorbtsiya i Poristost'. Trudy 4-oi Vsesoyuz. Konf. po Teoreticheskim Voprosam Adsorbtsii, Leningrad, 29 Yanvarya – 2 Fevralya 1974 g.* (Adsorption and Porosity. Proc. of the 4th All-Union. Conf. on Theoretical Issues of Adsorption, Leningrad, January 29 – February 2, 1974) (Moscow: Nauka, 1976)
78. Ehrlich G, in *Molecular Processes in Adsorption on Metals. Trans. 8th Natl. Vacuum Symp. 1961* (Oxford: Pergamon Press, 1962) p. 126
79. Redhead P A, Hobson J P, Kornelson E V *The Physical Basis of Ultrahigh Vacuum* (London: Chapman and Hall, 1968)
80. Cherepnin V N *Sorbtsionnye Yavleniya v Vakuumnoi Tekhnike* (Sorption Phenomena in Vacuum Technique) (Moscow: Sovetskoe Radio, 1973)
81. Inghram G M, Hayden R J, Hess D C, in *Mass Spectrometry in Physic Research. Proc.s of the NBS Semicentennial Symp. on Mass Spectroscopy in Physics Research, September 6–8, 1951* (National Bureau of Standards Circular, Vol. 522) (Washington, DC: National Bureau of Standards, 1953) p. 257
82. Dukel'skii V M, Zandberg E Ya *Zh. Eksp. Teor. Fiz.* **19** 73 (1949)
83. Berry H W *Phys. Rev.* **74** 848 (1948)
84. Stier P M, Barnett C F, Evans G E *Phys. Rev.* **96** 973 (1954)
85. Akishin A I *Sov. Phys. Usp.* **1** 113 (1958); *Usp. Fiz. Nauk* **66** 331 (1974)
86. Zalkind V M, Sushko I S, Tarasenko V P *Prib. Tekh. Eksp.* (5) 110 (1982)
87. Gusev V B, Polenov B V, Khazanov B I, in *Yadernoe Priborostroenie. Trudy Soyuz. Nauchno-Issledovatel'skogo Instituta Priborostroeniya* (Nuclear Instrumentation Engineering. Proc. of the Union

Scientific Research Institute of Instrumentation Engineering) Issue 8 (Moscow: Atomizdat, 1968)

88. Balashova N A, Merkulova N S, in *Izuchenie Spetsificheskoi Adsorbtsii Ionov i Polozheniya Tochki Nulevogo Zaryada Metodom Mechennykh Atomov. Trudy 4-go Soveshchaniya po Elektrokhimii* (Analysis on Specific Ion Adsorption and Zero Charge Point Position by the Marked Atom Method. Proc. of the 4th Meeting on Electrochemistry) (Moscow: AN SSSR, Otd. Khim. Nauk, 1950)
89. Vol'kenshtein F F, Kogan Sh M *Izv. Akad. Nauk Otd. Khim. Nauk* **9** 1536 (1959)